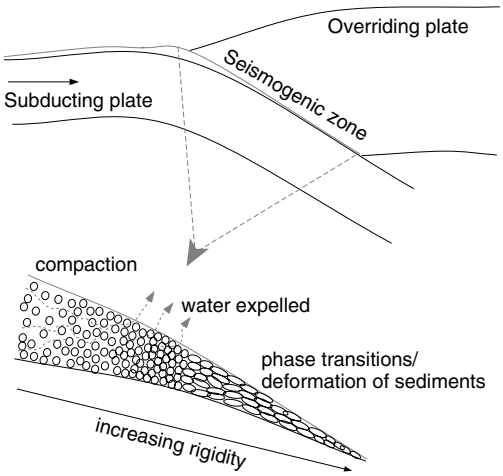

Figure 4 Generalized diagram of a subduction zone, with an expanded-scale view of the seismogenic-zone interface. As the high-porosity and unlithified sediments are subducted, they undergo several changes that can alter their rigidity. Increased pressure with depth causes compaction of the subducting sediments, expulsion of fluids, metamorphism, and mineralogical phase changes, resulting in higher rigidity of the material with increasing depth. Using our data to look at the rigidity variation end-member model, we have begun to quantify the magnitude of the changes of mechanical properties that occur with depth in the subduction zone.

illite transition, which occurs at temperatures of approximately 100–110 °C and depths of a few kilometres, depending on subduction convergence rates[22], is one such phase transition expected in the subducted sediments. The change from smectite, a weaker hydrated clay, to illite, a much stronger, dehydrated clay could lead to increased rigidities with increasing depths. Another phase transition occurring within subducting oceanic crust involves metamorphosis of basalt to eclogite, with an expulsion of fluid during the breakdown of water-bearing clays and amphiboles[23]. These phase transitions may play a role in changing the overall properties of the subduction-zone interface; however, our rigidity estimates involve a volumetric averaging of material in the seismogenic zone, so a variety of different mechanisms may contribute to the pattern in Fig. 3.

The model of rigidity variation with depth is particularly important in light of the occurrence of tsunami earthquakes, which produce unusually strong tsunamis for their seismic moment[3]. Several mechanisms have been proposed to account for tsunami earthquakes, including submarine landslides and earthquake rupture through low-rigidity sediments, either along the interface between the plates or within the forearc prism above the interface. For those events for which submarine landslides have been ruled out as the cause, earthquake source studies have shown that the rupture tends to occur at very shallow depths near the otherwise aseismic forearc wedge, where low-rigidity sediments are likely to be concentrated[24]. Tsunami earthquakes, such as the 1992 Nicaragua event, have been found to typically have anomalously slow rupture velocities, suggesting that low-rigidity material controls the rupture[25]. Reconciling the displacements needed to excite the Nicaragua tsunami with the observed seismic moment leads to rigidities 3–4 times lower than in PREM[26] and very close to those shown in Fig. 3. Similar modelling of the 1996 Peru tsunami also resulted in a smaller-than-average rigidity value to fit the tsunami run-up data[27]. These tsunami events can be seen as the natural consequences of ubiquitous depth dependence of rigidity in seismogenic zones. Our results indicate that for the constant-stress-drop model, analysis of rigidity variations in different zones based on small events can guide assessment of potential for tsunami earthquakes, along with improving the accuracy of slip estimates made for interplate faulting which underlie most earthquake probability calculations. □

Received 16 February; accepted 22 June 1999.

1. Kanamori, H. Rupture process of subduction-zone earthquakes. *Annu. Rev. Earth Planet. Sci.* **14,** 293–322 (1986).
2. Scholtz, C. *The Mechanics of Earthquakes and Faulting* (Cambridge Univ. Press, 1990).
3. Kanamori, H. Mechanism of tsunami earthquakes. *Phys. Earth Planet. Inter.* **6,** 246–259 (1972).
4. Fukao, Y. Tsunami earthquakes and subduction processes near deep sea trenches. *J. Geophys. Res.* **84,** 2303–2314 (1979).
5. Pelayo, A. M. & Wiens, D. A. Tsunami earthquakes: slow thrust faulting events in the accretionary wedge. *J. Geophys. Res.* **97,** 15321–15337 (1992).
6. Bilek, S. L. & Lay, T. Variation of interplate fault zone properties with depth in the Japan subduction zone. *Science* **281,** 1175–1178 ('998).
7. Bilek, S. L. & Lay, T. Comparison of depth dependent fault zone properties in the Japan trench and Middle America trench. *Pure Appl. Geophys.* (in the press).
8. Ruff, L. J. Multi-trace deconvolution with unknown scale factors: omnilinear inversion of P and S waves for source time functions. *Geophys. Res. Lett.* **16,** 1043–1046 (1989).
9. Tichelaar, B. W. & Ruff, L. J. Seismic coupling along the Chilean subduction zone. *J. Geophys. Res.* **96,** 11997–12022 (1991).
10. Ruff, L. J. & Miller, A. D. Rupture process of large earthquakes in the northern Mexico subduction zone. *Pure Appl. Geophys.* **142,** 101–171 (1994).
11. Christensen, D. H. & Ruff, L. J. Analysis of the trade-off between hypocentral depth and source time function. *Bull. Seismol. Soc. Am.* **75,** 1637–1656 (1985).
12. Kanamori, H. & Anderson, D. L. Theoretical basis of some empirical relations in seismology. *Bull. Seismol. Soc. Am.* **65,** 1073–1095 (1975).
13. Vidale, J. E. & Houston, H. The depth dependence of earthquake duration and implications for rupture mechanics. *Nature* **35,** 45–47 (1993).
14. Ekstrom, G. & Engdahl, E. R. Earthquake source parameters and stress distribution in the Adak Island region of the central Aleutian Islands, Alaska. *J. Geophys. Res.* **94,** 15499–15519 (1989).
15. Houston, H., Benz, H. M. & Vidale, J. E. Time functions of deep earthquakes from broadband and short-period stacks. *J. Geophys. Res.* **103,** 29895–29913 (1998).
16. Plank, T. & Langmuir, C. H. The chemical composition of subducting sediment and its consequences for the crust and mantle. *Chem. Geol.* **145,** 325–394 (1998).
17. von Huene, R. & Scholl, D. W. Observations at convergent margins concerning sediment subduction, subduction erosion, and the growth of continental crust. *Rev. Geophys.* **29,** 279–316 (1991).
18. Tera, F. *et al.* Sediment incorporation in island-arc magmas: Inferences from ^{10}Be. *Geochim. Cosmochim. Acta* **50,** 535–550 (1986).
19. Kimura, G. *et al. Proc. ODP Init. Rep.* Costa Rica accretionary wedge. **170,** 1–458 (1997).
20. von Huene, R. & Lallemand, S. Tectonic erosion along the Japan and Peru convergent margins. *Geol. Soc. Am. Bull.* **102,** 704–720 (1990).
21. Suyehiro, K. & Nishizawa, A. Crustal structure and seismicity beneath the forearc off northwestern Japan. *J. Geophys. Res.* **99,** 22331–22347 (1994).
22. Vrolijk, P. On the mechanical role of smectite in subduction zones. *Geology* **18,** 703–707 (1990).
23. Peacock, S. M. The importance of blueschist–eclogite dehydration reactions in subducting oceanic crust. *Geol. Soc. Am. Bull.* **105,** 684–694 (1993).
24. Ihmlé, P. F., Gomez, J.-M., Heinrich, P. & Guibourg, S. The 1996 Peru tsunamigenic earthquake: broadband source process. *Geophys. Res. Lett.* **25,** 2691–2694 (1998).
25. Kanamori, H. & Kikuchi, M. The 1992 Nicaragua earthquake: a slow tsunami earthquake associated with subducted sediments. *Nature* **361,** 714–716 (1993).
26. Satake, K. Mechanism of the 1992 Nicaragua tsunami earthquake. *Geophys. Res. Lett.* **21,** 2519–2522 (1994).
27. Heinrich, P., Schindelé, F., Guibourg, S. & Ihmlé, P. M. Modeling of the February 1996 Peruvian tsunami. *Geophys. Res. Lett.* **25,** 2687–2690 (1998).
28. Tichelaar, B. W. & Ruff, L. J. Depth of seismic coupling along subduction zones. *J. Geophys. Res.* **98,** 2017–2037 (1993).
29. Dziewonski, A. M. & Anderson, D. L. Preliminary reference Earth model. *Phys. Earth Planet. Inter.* **25,** 297–356 (1981).

Supplementary information is available on *Nature*'s World-Wide Web site (http://www.nature.com) or as paper copy from the London editorial office of *Nature*.

Acknowledgements. Data were obtained through the IRIS datacenter. This work was supported by the US NSF. We thank S. Schwartz and E. Silver for comments on early drafts.

Correspondence and requests for materials should be addressed to S.B. (e-mail: sbilek@es.ucsc.edu).

Missing lithotroph identified as new planctomycete

Marc Strous*, John A. Fuerst†, Evelien H. M. Kramer*, Susanne Logemann*, Gerard Muyzer‡, Katinka T. van de Pas-Schoonen*, Richard Webb†, J. Gijs Kuenen* & Mike S. M. Jetten*

** Department of Biotechnology, Delft University of Technology, Julianalaan 67, 2628 BC Delft, The Netherlands*
† Department of Microbiology & Parasitology and the Centre for Microscopy and Microanalysis, University of Queensland, Brisbane, Queensland 4072, Australia
‡ Netherlands Institute for Sea Research, 1790 AB Den Burg, The Netherlands

With the increased use of chemical fertilizers in agriculture, many densely populated countries face environmental problems associated with high ammonia emissions. The process of anaerobic ammonia oxidation ('anammox') is one of the most innovative technological advances in the removal of ammonia nitrogen from

waste water[1,2]. This new process combines ammonia and nitrite directly into dinitrogen gas[3]. Until now, bacteria capable of anaerobically oxidizing ammonia had never been found and were known as "lithotrophs missing from nature"[4]. Here we report the discovery of this missing lithotroph and its identification as a new, autotrophic member of the order *Planctomycetales*, one of the major distinct divisions of the Bacteria[5]. The new planctomycete grows extremely slowly, dividing only once every two weeks. At present, it cannot be cultivated by conventional microbiological techniques. The identification of this bacterium as the one responsible for anaerobic oxidation of ammonia makes an important contribution to the problem of unculturability.

For over a century, microbiologists have generally acknowledged Koch's postulate that to prove that a process such as the anaerobic oxidation of ammonia is mediated by a bacterium, this bacterium should be isolated in pure culture and still be able to reproduce the process. But for the past ten years, the anammox process has resisted such meaningful microbiological characterization.

Electron microscopy provided an incentive to continue pursuing the quest for the bacterium responsible for anammox, because a peculiar morphotypical microorganism dominated the multispecies biofilms that mediated the process. Thin sectioning of cryosubstituted material revealed that cells of this morphotype were characteristically compartmented in their internal ultrastructure (Fig. 1a). Such membrane-bounded cell compartments were so far found only in cultured strains of the order *Planctomycetales*[6,7]. When cell surfaces were examined by negative staining (Fig. 1b), the anammox morphotype displayed uniformly distributed crateriform structures, circular electron-dense areas known to be characteristic of planctomycetes[8].

It would be surprising if a planctomycete was responsible for anammox. The order *Planctomycetales*—comprising a separate major division of the Bacteria—has been represented so far only by a few organotrophs[8]. Formerly the planctomycetes were considered to be of limited environmental importance. But this view is changing rapidly as molecular microbial ecology repeatedly provides new evidence showing that these bacteria are ubiquitous and make up a substantial portion of the natural bacterial population[9–13]. The recognition of the planctomycetes as a major bacterial division may change our notion of what bacteria are. Planctomycetes have single- or double-membrane-bounded compartments (see above and Fig. 1) separating their chromosome from the remainder of the cytoplasm[6,7]. They lack peptidoglycan in their cell walls and are insensitive to ampicillin[14,15].

As conventional purification using single-cell isolation had failed, we physically purified the morphotypical microorganism from the multispecies biofilms[16] by density-gradient centrifugation. The purification procedure consisted of three steps: (1) disruption of the biofilms by mild sonication; (2) separation of the single cells obtained and the remaining biofilm fragments; and (3) purification of the single cells using Percoll density-gradient centrifugation (Table 1).

We showed that the purified cells were responsible for anaerobic ammonium oxidation by incubating the obtained cell suspensions (99.6% pure) with the substrates ammonium and nitrite (5 mM each) and measuring substrate consumption over time.

Surprisingly, it seemed that both the purified and unpurified cells were only active when the cell concentration was higher than

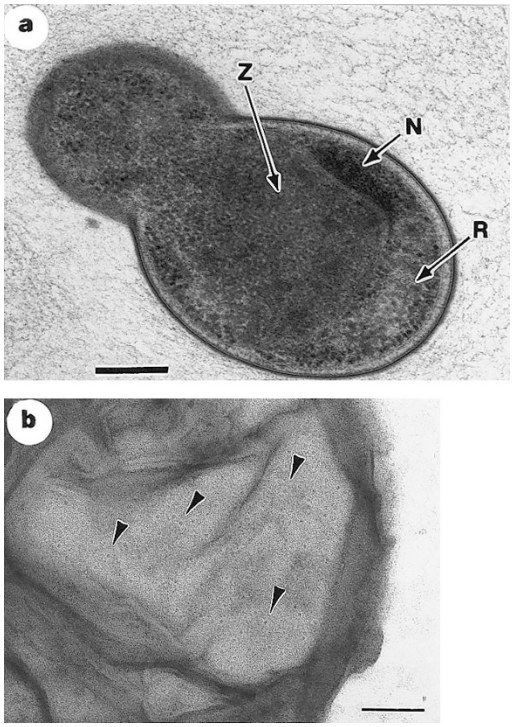

Figure 1 Transmission electron micrograph of anammox biofilms. **a**, Thin-sectioned cell of dominant morphotype from the anammox biofilm enrichment culture, demonstrating unusual compartmentalized internal organization and budding reproduction. The mother cell of the budding cell shown possesses a central membrane-bounded ribosome-free zone (Z), surrounded by a membrane-bounded ribosome-rich region (R) in which the fibrillar nucleoid (N) is situated. Bar marker is 0.2 μm. **b**, Portion of the surface of a negatively stained cell of dominant morphotype from the same culture, displaying uniformly distributed, circular crateriform structures, examples of which are indicated by arrows. Bar marker is 100 nm.

10^{10}–10^{11} cells ml^{-1}. This was not noticed previously because we had studied anammox only in biofilms, where the cell density is naturally very high. One might argue that the high concentrations of purified cells were required to attain a sufficient amount of contaminating microorganisms required for anammox activity. However, this possibility could be eliminated because control experiments showed that the activity of unpurified cells was also density dependent (Table 1). Therefore, we concluded that the cell density of the anammox morphotype was important, and not the amount of contaminants. It is as yet unclear whether the density-dependent activity of these cells results from cell-to-cell communication through homoserine lactone autoinducers (quorum sensing)[17] or whether a different mechanism is responsible for the density dependency in this case.

Because the Percoll purification procedure yielded only a small number of cells (Table 1), the anaerobic activity test was miniaturized to 30–40 μl to attain high cell densities. In addition to the required high cell concentration, the cells needed to be supplied with a trace amount of one of the anammox intermediates hydrazine or hydroxylamine (100 μM) before they became active, and the nitrite

Table 1 Purification and cell-density-dependent activity of anammox cells from anammox biofilms

Purification step	Purity* (%)	Total yield of bacterial cells (mg protein)	Specific activity* (nmol NH_4^+ per mg protein per min)	Cell density threshold (cells per ml)
Mixed culture biofilms	70 ± 10	50	25 ± 5	10^7–10^9†
Single cells from sonicated biofilms	85 ± 5	2	20 ± 4	10^{10}–10^{11}
Purified cell suspension after density gradient centrifugation	99.6 ± 0.2	0.5	18 ± 3	10^{10}–10^{11}

*Values are expressed as mean ± standard deviation.
† Average of biofilms and culture liquid. Inside the biofilms, cells were densely packed, leading to local cell densities of at least 10^{10}–10^{11} ml^{-1}.

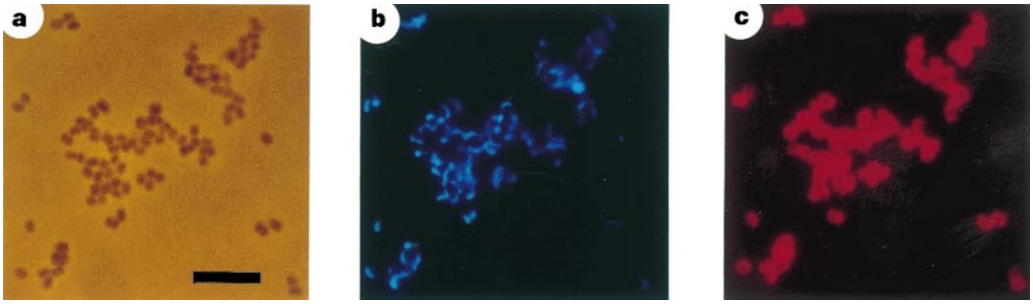

Figure 2 Fluorescent *in situ* hybridization of purified anammox cells. Identical field viewed by: **a**, phase contrast microscopy; **b**, epifluorescence microscopy with cells stained with the general DNA stain DAPI; and **c**, epifluorescence after hybridization with anammox organism 16S rRNA-sequence based, Cy3-labelled probe S-G-Amx-1015-a-A-18 (5′-GAT ACC GTT CGT CGC CCT-3′) at 20% (v/v) formamide. Bar marker is 5 μm.

concentration needed to be lower than 5 mM to prevent substrate inhibition.

The high cell density and the low substrate concentration allowed the purified cells only a brief burst of activity, little more than 100 catabolic cycles (each cell consumed only a small amount of substrate, every individual enzyme turning over 100 times at most). Nethertheless, the activity of the purified cells was only slightly lower than the activity of the biofilms (Table 1) and the stoichiometry of the conversion was identical: 1.3 moles of nitrite were consumed and 0.2 moles of nitrate were produced per mole of ammonium consumed. Even assimilation of CO_2 by the anaerobic ammonium-oxidizing cells could be measured. During the experiment, the stoichiometry of ^{14}C-CO_2 incorporation increased rapidly from 0 to 20 millimoles of CO_2 per mole of ammonium consumed. In control experiments with unpurified cell suspensions prepared from enrichment culture biofilms, the rate of CO_2 incorporation was always less. The pathway of CO_2 assimilation is not yet resolved but the recorded ribulose bisphosphate carboxylase activity in the biofilm enrichment culture was less than 50% of the activity required to account for the measured CO_2 incorporation. Alternatively, one of the other four known autotrophic pathways might be present in this case. Up until now, planctomycetes were known as organotrophic organisms (that is, incapable of autotrophic CO_2 fixation) and their biochemical pathways are so far unexplored.

Because the responsible bacterium was purified but not isolated, contaminating organisms might contribute to the observed activity. However, from kinetic and stoichiometric perspectives it is extremely unlikely that the contaminating organisms (1 in 200) contribute significantly to anammox catabolism or anabolism. However, it is quite possible that other organisms are required for growth of the anammox organism. Possible symbionts might, for example, supply growth factors and scavenge by-products of anammox anabolism.

To determine the phylogenetic identity of the purified cells, we extracted DNA and RNA from the purified suspensions and amplified the 16S ribosomal RNA gene directly using polymerase chain reaction or indirectly after reverse transcription of RNA (RT-PCR) from complementary DNA obtained from the 16S rRNA itself. Although the cell suspensions were more than 99% pure, only the RT-PCR-derived clone libraries were dominated (80%) by a single sequence. Based on this sequence we designed 18 specific oligonucleotide probes, labelled with Cy3 fluorochrome for fluorescent *in situ* hybridization (FISH). Ten of these probes gave bright and specific hybridization signals with the purified morphotypical microorganism (Fig. 2). Combined FISH and 4,6-diamidino-2-phenylindole (DAPI) staining confirmed the internal cell compartmentalization. The FISH signal was ring shaped, indicating the absence of ribosomes in the inner cell compartment. The DAPI signal, staining the genomic DNA, was concentrated in a half-ring, which is consistent with the localization of the nucleoid in Fig. 1a.

The 16S rRNA sequence of the anammox organism (1,453 base pairs, from position 7 to 1,390; *Escherichia coli* numbering) was aligned and analysed phylogenetically with other bacterial 16S rRNA sequences[18]. The anammox organism was identified as a deep-branching planctomycete (Fig. 3), most closely related to a sequence amplified from a marine snow aggregate[19] (sequence identity 80.2%). Sequence identity with other planctomycetes was 74–77%. The new sequence of the 16S rRNA gene shared most but not all signature positions with those of the other planctomycetes[8,20,21], confirming its position as a deep-branching but still related sequence.

Finally, the missing link in the biogeochemical nitrogen cycle seems to have been found; it is an organism in the order *Planctomycetales,* a distinctive division of the domain Bacteria, with unique cell organization and cell walls, large evolutionary distances and few cultivated representatives.

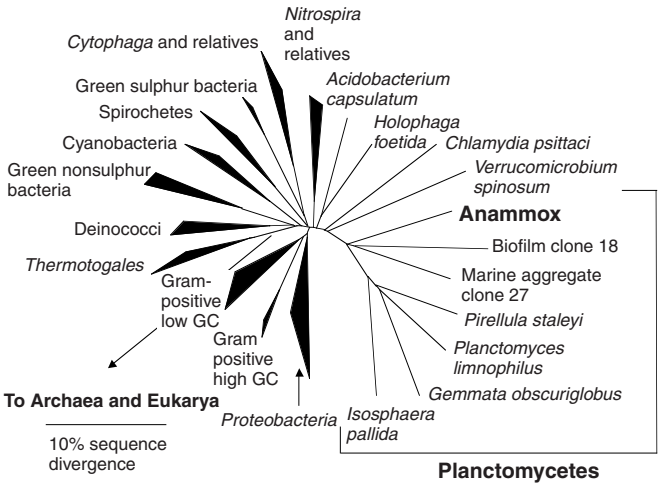

Figure 3 Phylogenetic position of the lithotroph responsible for anaerobic ammonium oxidation within the domain Bacteria, based on 16S rRNA phylogeny. The anammox bacterium represents a new, deep branch inside the order *Planctomycetales*.

Methods

Purification and activity. Biofilms[16] were washed and concentrated in 40 ml HEPES/bicarbonate buffer (70/10 mM, pH 7.8), sonicated in 5 ml portions (150 W, 30 s, 18-mm tip width) and, after centrifugation (10,000*g*, 5 min), an upper orange pellet containing undisrupted biofilm fragments was separated from the lower red pellet containing the single cells. After washing in the same buffer, the single-cell fraction was purified using Percoll centrifugation (6.9 ml Percoll (Pharmacia) and 3.1 ml cell suspension; centrifugation at 10,000*g* for 60 min at 5 °C; Sorval SS34 fixed angle rotor). A broad, red band of target cells in the lower half of the tube was extracted and washed in sterile buffer (see above). Anammox activity was tested in a 30-μl activity test in anaerobic containers

(same buffer containing 4.5 mg protein ml^{-1} (10^{10}–10^{11} cells ml^{-1}), 5 mM ammonium and nitrite, 100 μM hydrazine) and consumption of ammonium and nitrite and production of nitrate and incorporation of ^{14}C-CO_2 was measured as described previously[16,22]. Purity was assessed by microscopic counting, electron microscopy and FISH.

Electron microscopy. Pelleted cell flocs were processed by a cryosubstitution protocol before embedding, sectioning and section staining, all using methods described in ref. 7. Cells were negatively stained using 1% uranyl acetate + 0.4% sucrose, after dispersal of flocs.

Fluorescent microscopy. FISH and DAPI staining were done as described[10]. Formamide concentration versus specificity of all probes was determined with the appropriate reference organism for each probe and with the biofilm enrichment culture and several undefined, heterogeneous environmental samples. All probes were at least 18 nucleotides long.

Phylogeny. Treeing and phylogenetic analysis was done using the ARB software package[18]. The sequence was obtained after DNA isolation, PCR amplification (primers 27 or 519 forward and 1,390 reverse; annealing at 46 °C, melting at 94 °C, 30 cycles), ligation of the product in vector pGEMT (Promega) and transformation into competent DH5α *E. coli* cells. The clone library was screened using restriction digestion, and representative clones of each restriction pattern were sequenced. The anammox sequence (GenBank accession number AJ131819) always grouped with the other planctomycete sequences, independent of treeing algorithm (neighbour joining, distance matrix or parsimony), inclusion of other bacterial phyla in the tree or the choice of the outgroup (*Thermotoga, Aquifex* or the Archaea).

Received 4 May; accepted 1 June 1999.

1. Jetten, M. S. M., Horn, S. J. & van Loosdrecht, M. C. M. Towards a more sustainable wastewater treatment system. *Wat. Sci. Tech.* **35,** 171–180 (1997).
2. Strous, M., Van Gerven, E., Ping, Z., Kuenen, J. G. & Jetten, M. S. M. Ammonium removal from concentrated waste streams with the anaerobic ammonium oxidation process. *Water Res.* **31,** 1955–1962 (1997).
3. Van de Graaf, A. A., de Bruin, P., Robertson, L. A., Jetten, M. S. M. & Kuenen, J. G. Metabolic pathway of anaerobic ammonium oxidation on basis of ^{15}N-studies in a fluidized bed reactor. *Microbiology* **143,** 2415–2421 (1997).
4. Broda, E. Two kinds of lithotrophs missing in nature. *Z. Allgem. Mikrobiol.* **17,** 491–493 (1977).
5. Schlesner, H. & Stackebrandt, E. Assignment of the genera *Planctomyces* and *Pirella* to a new family *Planctomycetaceae* fam. nov. and description of the order *Planctomycetales* ord. nov. *Syst. Appl. Microbiol.* **8,** 174–176 (1986).
6. Fuerst, J. A. & Webb, R. I. Membrane-bounded nucleoid in the eubacterium *Gemmata obscuriglobus*. *Proc. Natl Acad. Sci. USA* **88,** 8184–8188 (1991).
7. Lindsay, M. R., Webb, R. I. & Fuerst, J. A. Pirellulosomes: a new type of membrane-bounded cell compartment in planctomycete bacteria of the genus *Pirellula*. *Microbiology* **143,** 739–748 (1997).
8. Fuerst, J. A. The planctomycetes: emerging models for microbial ecology, evolution and cell biology. *Microbiology* **141,** 1493–1506 (1995).
9. Vergin, K. L. *et al.* Screening of a fosmid library of marine environmental genomic DNA fragments reveals four clones related to members of the order *Planctomycetales*. *Appl. Environ. Microbiol.* **64,** 3075–3078 (1998).
10. Neef, A., Amann, R. I., Schlesner, H. & Schleifer, K. H. Monitoring a widespread bacterial group: in situ detection of planctomycetes with 16S rRNA-targeted probes. *Microbiology* **144,** 3257–3266 (1998).
11. Hugenholtz, P., Goebel, B. M. & Pace, N. R. Impact of culture-independent studies on the emerging phylogenetic view of bacterial diversity. *J. Bacteriol.* **180,** 4765–4774 (1998).
12. Byers, H. K., Stackebrandt, E., Hayward, C. & Blackall, L. L. Molecular investigation of a microbial mat associated with the Great Artesian Basin. *FEMS Microbiol. Ecol.* **25,** 391–403 (1998).
13. Zarda, B. *et al.* Analysis of bacterial community structure in bulk soil by in situ hybridization. *Arch. Microbiol.* **168,** 185–192 (1997).
14. Liesack, W., König, H., Schlesner, H. & Hirsch, P. Chemical composition of the peptidoglycan-free cell envelopes of budding bacteria of the *Pirella/Planctomyces* group. *Arch. Microbiol.* **145,** 361–366 (1986).
15. König, E., Schlesner, H. & Hirsch, P. Cell wall studies on budding bacteria of the *Planctomyces/Pasteuria* group and on a *Prosthecomicrobium* sp. *Arch. Microbiol.* **138,** 200–205 (1984).
16. Strous, M., Heijnen, J. J., Kuenen, J. G. & Jetten, M. S. M. The sequencing batch reactor as a powerful tool for the study of slowly growing anaerobic ammonium oxidising microorganisms. *Appl. Microbiol. Biotechnol.* **50,** 589–596 (1998).
17. Fuqua, C. & Greenberg, E. Self perception in bacteria: quorum sensing with acylated homoserine lactones. *Curr. Opin. Microbiol.* **1,** 183–189 (1998).
18. Ludwig, W. *et al.* Bacterial phylogeny based on comparative sequence analysis. *Electrophoresis* **19,** 554–568 (1998).
19. Delong, E. F., Franks, D. G. & Alldredge, A. L. Phylogenetic diversity of aggregate-attached versus free-living marine bacterial assemblages. *Limnol. Oceanogr.* **38,** 924–934 (1993).
20. Fuerst, J. A. *et al.* Isolation and molecular identification of planctomycete bacteria from postlarvae of the giant tiger prawn *Penaeus monodon*. *Appl. Environ. Microbiol.* **63,** 254–262 (1997).
21. Woese, C. R. Bacterial evolution. *Microbiol. Rev.* **51,** 221–271 (1987).
22. Van de Graaf, A. A., Debruijn, P., Robertson, L. A., Jetten, M. S. M. & Kuenen, J. G. Autotrophic growth of anaerobic ammonium oxidizing microorganisms in a fluidized bed reactor. *Microbiology* **142,** 2187–2196 (1996).

Acknowledgements. We thank A. Raghoebarsing and J. Schalk for technical assistance; M. Wagner (TU Munich, Germany) for instruction on fluorescent *in situ* hybridization; and the Foundation of Applied Research (STW) for financial support. J.A.F. and R.W. acknowledge the support of the Australian Research Council.

Correspondence and requests for materials should be addressed to M.S.M.J. (e-mail: m.jetten@stm.tudelft.nl). The anammox sequence has been deposited in GenBank (accession no. AJ131819).

Sperm competition between *Drosophila* males involves both displacement and incapacitation

Catherine S. C. Price, Kelly A. Dyer* & Jerry A. Coyne

Department of Ecology and Evolution, The University of Chicago, 1101 East 57th Street, Chicago, Illinois 60637, USA

Females in almost all animal groups copulate with multiple males[1,2]. This behaviour allows different males to compete for fertilization[3] and gives females the opportunity to mediate this competition[4]. In many animals and most insects, the second male to copulate with a female typically sires most of her offspring[1,5,6]. In *Drosophila melanogaster*, this second-male sperm precedence has long been studied[7–15] but, as in most species, its mechanism has remained unknown. Here we show, using labelled sperm in doubly mated females, that males can both physically displace and incapacitate stored sperm from earlier-mating males. Displacement occurs only if the second male transfers sperm to the female, and in only one of her three sperm-storage organs. Incapacitation can be caused by either fertile or spermless second males, but requires extended intervals between matings. Sperm from different males are not 'stratified' in the storage organs but mix freely. Many animal species may have multiple mechanisms of sperm competition like those observed here, and revealing these mechanisms is necessary to understand the genetic and evolutionary basis of second-male sperm precedence in animals.

The consequences of multiple mating are well known in *D. melanogaster*. Females store sperm in a long tubular seminal receptacle and two mushroom-shaped spermathecae[10]. The proportion of offspring produced after the second mating that are sired by the second male, P_2, is typically above 0.8 in laboratory experiments[16]. Most wild-caught females carry sperm from multiple males[17], and females in nature may copulate when they still carry a sizeable sperm load from previous matings[18]. If a sperm-carrying female remates, she produces fewer offspring sired by the first male than she would have if she had not remated[16]. At least some of this reduction in first-male reproductive success occurs if the second male transfers only seminal fluid and no sperm[12,14]. Seminal fluid therefore plays some role in second-male sperm precedence[15], but the extent of this role is unclear because some studies[10,19] have not revealed a 'seminal-fluid effect'. To investigate this discrepancy, we looked for a seminal-fluid effect in experiments carried out at two different time intervals.

Rematings to fertile second males produced the usual result of second-male sperm precedence and resulted in significant reduction of first-male reproductive success when females remated after either two or seven days (Fig. 1a). When females were remated in exactly the same manner to infertile XO males transferring only seminal fluid (see Methods), there was a significant reduction in first-male offspring when females were remated after seven days, but only a slight and non-significant reduction when they were remated after two days (Fig. 1a). Similar results were found when this experiment was repeated with Ives males instead of bw^D males (carrying the brown-dominant mutation) as first mates (data not shown). These results confirm that at least some of the second male's precedence can be ascribed to his seminal fluid, and, because this effect was not seen until seven days after remating, indicate that first-male sperm

* Present address: Department of Biology, University of Rochester, Rochester, New York 14627, USA.